

A STATISTICAL DETERMINISTIC APPROACH TO HURRICANE RISK ASSESSMENT

BY KERRY EMANUEL, SAI RAVELA, EMMANUEL VIVANT, AND CAMILLE RISI

In a novel approach to hurricane wind risk assessment, a coupled ocean–atmosphere hurricane model is run along each of a large number of hurricane tracks synthesized by two independent methods.

Hurricanes are among the most lethal and costly natural disasters affecting mankind. The Galveston, Texas, hurricane of 1900 was the deadliest natural catastrophe in U.S. history, and only a few years ago, in 1998, Hurricane Mitch killed upward of 11,000 in Central America. While the loss of life in the more developed countries has been greatly reduced by a highly successful program of warnings, evacuations, and advanced building construction and regulation, property losses are

escalating rapidly owing to accelerated construction in hurricane-prone areas. Thus, Hurricane Katrina of 2005 was the single most costly natural disaster in U.S. history, incurring more than \$125 billion in losses, while it has been estimated that were the 1926 Miami, Florida, hurricane to strike today it would do more than \$76 billion in damage (Pielke and Landsea 1998).

In some cases, such as Hurricane Mitch, much of the death toll and property losses result from freshwater flooding produced by torrential rains. Unfortunately, quantitative understanding of hurricane-related precipitation, particularly over mountainous terrain, has not advanced to the point of yielding reliable precipitation forecasts, nor are historical records of hurricane-induced rainfall extensive enough to make meaningful estimates of flooding risks. But, the record of hurricane wind speeds is much more complete and, historically, much of the damage and loss of life results from hurricane winds and wind-induced storm surges. This has led to several efforts to assess risks associated with hurricane winds. A comprehensive review of wind loss modeling is provided by Watson and Johnson (2004); here, we undertake a brief overview.

AFFILIATIONS: EMANUEL, RAVELA, VIVANT, AND RISI—Program in Atmospheres, Oceans, and Climate, Massachusetts Institute of Technology, Cambridge, Massachusetts

A supplement to this article is available online (DOI:10.1175/BAMS-87-3-Emanuel)

CORRESPONDING AUTHOR: Kerry Emanuel, Room 54-1620, MIT, 77 Massachusetts Avenue, Cambridge, MA 02139
E-mail: emanuel@texmex.mit.edu

The abstract for this article can be found in this issue, following the table of contents.

DOI:10.1175/BAMS-87-3-299

In final form 16 September 2005
©2006 American Meteorological Society

All current estimation techniques begin with historical compilations of hurricane tracks and intensities, such as the so-called “best track” data compilations maintained by forecasting operations such as the National Oceanic and Atmospheric Administration’s (NOAA’s) Tropical Prediction Center (TPC) and the U.S. Navy’s Joint Typhoon Warning Center (JTWC). The records typically contain the storm center position every 6 h, together with a single intensity estimate (maximum wind speed and/or central pressure) every time period. Early risk assessments (e.g., Georgiou et al. 1983; Neumann 1987) fitted standard distribution functions, such as lognormal or Weibull distributions, to the distribution of maximum intensities of all historical storms coming within a specified radius of the point of interest, and then, drawing randomly from such distributions, used standard models of the radial structure of storms, together with translation speed and landfall information, to estimate the maximum wind achieved at the point of interest. A clear drawback of this approach is that estimates of the frequency of high-intensity events are sensitive to the shape of the tail of the assumed distribution, for which there is very little supporting data. This limitation was, to some extent, circumvented in the work of Darling (1991) and Chu and Wang (1998), who used empirical global distributions of relative intensity (the ratio of actual to potential intensity¹) together with the climatology of potential intensity to infer local intensity distributions. A similar approach was taken by Murnane et al. (2000), who used global estimates of hurricane actual (rather than relative) wind intensity cumulative probability distributions. A somewhat different tack was taken by Vickery et al. (2000), who used statistical properties of historical tracks and intensities to generate a large number of synthetic storms in the North Atlantic basin. Six-hour changes in direction, translation speed, and intensity along each track were modeled as linear functions of previous values of those quantities as well as position and sea surface temperature. A similar approach was taken by Casson and Coles (2000), though they generated synthetic tracks by randomly perturbing historical tracks, and simulated intensity along each track by drawing randomly from the whole collection of

historical tracks over water. We follow Vickery et al. (2000) in generating large numbers of tracks, but use different techniques to accomplish this.

Most of the aforementioned wind risk assessment methods rely directly on historical hurricane-track data to estimate the frequency of storms passing close to points of interest, and must assume that the intensity evolution is independent of the particular track taken by the storm [though Darling (1991) accounts for the time elapsed after storm formation]. Moreover, the relative intensity method must fail when storms move into regions of small or vanishing potential intensity, as they often do in the western North Atlantic. Return-period estimation is particularly problematic in places like New England, which have experienced infrequent but enormously destructive storms, but for which the historical record is sparse and the local potential intensity is zero.

COMBINING STATISTICAL TRACK GENERATION WITH DETERMINISTIC INTENSITY MODELING.

As a step toward circumventing some of these difficulties, we developed two largely independent techniques for generating large numbers of synthetic hurricane tracks, along each of which we run a deterministic, coupled numerical model to simulate storm intensity. The two track generation techniques are described in detail in appendixes A and B, respectively, and the deterministic intensity model is reviewed in appendix C. Here, we provide a brief overview.

Both track methods originate storm tracks by a random draw from a space–time probability density function of genesis locations based on a compilation of historical genesis points derived from tropical cyclone best-track data, as described in detail in the “Synthetic track generation using Markov chains” section of the online supplement to this paper (DOI: 10.1175/BAMS-87-3-Emanuel). For this purpose, we used best-track data during and after 1970, which is the first year we consider the global satellite detection of tropical cyclones to be complete.

The first track generation technique begins with certain key statistical features of historical hurricane tracks, including the spatiotemporal distribution of genesis and storm motion, and then generates synthetic tracks taking 6-h steps and using a Markov chain²

¹ The maximum wind speed theoretically attainable in tropical cyclones given the large-scale thermodynamic conditions (e.g., see Emanuel 2000).

² A Markov chain is a sequence of random values whose probabilities at a time interval depend upon the value of the number at the previous time. A simple example is the nonreturning random walk.

for each 6-h displacement. In this Markov process, each 6-h step depends both on the properties of the last step and on the climatological probability distribution of rates of change of displacement in direction at the current position and time. By this means, the tracks conform to the observed statistics (as a function of space and time) of the motion of historical hurricanes while preserving memory of their previous motion. The key variables in this technique are the translation speed and direction, and their rates of change over 6 h. Details may be found in appendix A. For this purpose, we use historical hurricane data over the whole period of record, because we believe that observed storm movement is somewhat less problematic than storm origin locations in the presatellite era. A comparison of the 6-h displacement statistics from tracks generated this way with observed displacement statistics is shown in Fig. 1.

Among the many processes that influence hurricane intensity is the vertical shear of the environmental wind, and it is therefore necessary to account for varying wind shear to model realistic variations in hurricane intensity. A drawback of the Markov track generation method is that, when it comes time to model storm intensity along each track, one must assume that the track and the shear are largely independent. This drawback could be circumvented, to a degree, by using reanalysis data to develop statistical relationships between historical hurricane tracks and environmental wind. Another approach, which forms the basis of our second track technique, is to generate tracks and shear from the same synthetic wind fields. This may be possible, because, to a first approximation, hurricanes move with some weighted vertical mean of the environmental flow in which

they are embedded (Holland 1983) plus a “beta drift,” owing to the effect of the vortex flow on the ambient potential vorticity distribution (Davies 1948; Rossby 1949). The National Hurricane Center runs a simple model based on this principle, the “beta and advection model” (Marks 1992). Using this technique, we can create tracks and environmental wind that are mutually consistent. Note that for the present purpose, it is not necessary for the track generator to also be a good track forecast model, as long as it is not biased.

Thus, our second synthetic track method, which also generates storms as a random draw from the collection of historical genesis points, moves the storms according to a weighted average of the

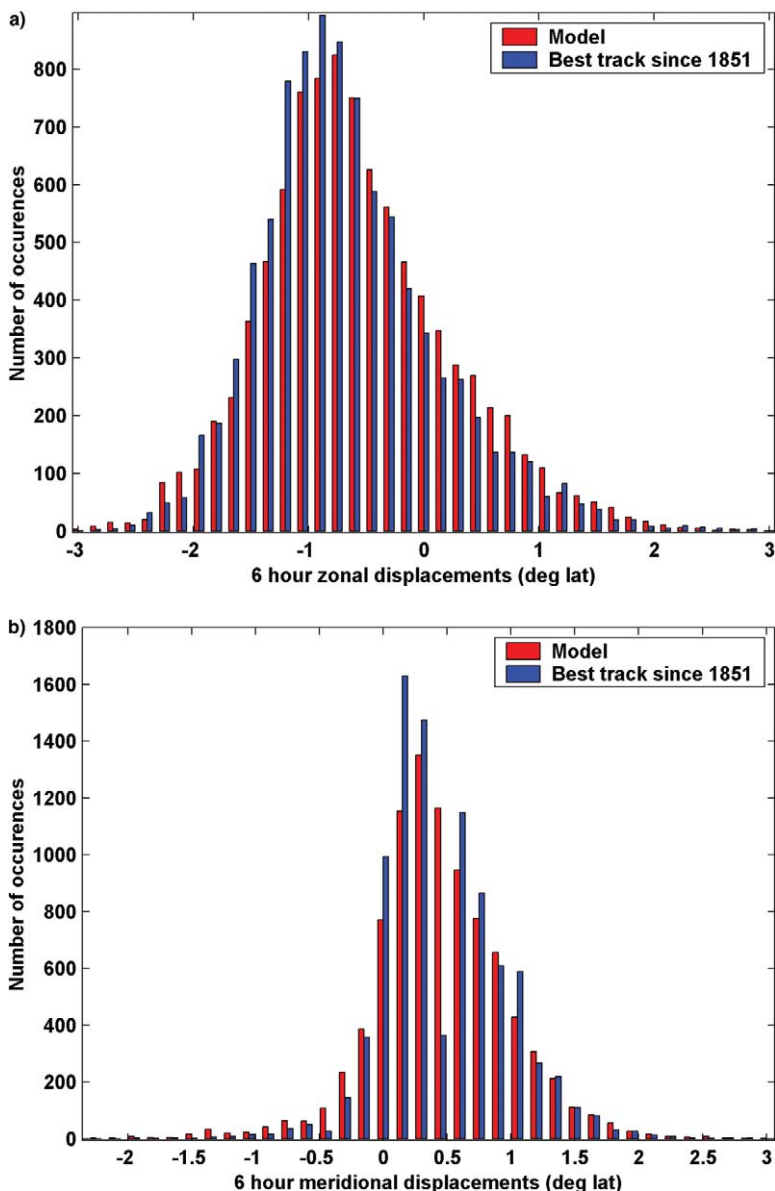


FIG. 1. Histograms of observed (blue) and modeled (red) frequency distributions of 6-h (a) zonal and (b) meridional displacements for a region of the North Atlantic bounded by 10° and 30°N and 80° and 30°W; 1,000 tracks from method 1 were used.

ambient flow at 850 and 250 hPa, plus a constant³ beta-drift correction, as detailed in appendix B. The ambient flow varies randomly in time, but it is constructed so that its mean, variance, and covariances conform to monthly mean climatologies derived from the National Centers for Environmental Prediction (NCEP)–National Center for Atmospheric Research (NCAR) reanalysis dataset, and so that its kinetic energy follows the ω^{-3} power

law of geostrophic turbulence. The 6-h displacement statistics from tracks generated using this method are compared to observations in Fig. 2.

As we shall see in the next section, each track method has advantages and disadvantages, and using both methods helps assess the overall quality of our hurricane risk assessment.

Once a synthetic track is produced by either method, it is then necessary to estimate the evolution of storm intensity along the track. In principle, one could use a Markov chain process to do this, making each increment of intensity (e.g., maximum wind speed) conditional on storm position, previous intensities, etc., as determined from historical storm data. A good way to do this would be in terms of relative intensity, pioneered by Darling (1991), with the climatological distributions as in Emanuel (2000). While such a procedure might work quite well in data-rich regions, the paucity of data in other regions (e.g., New England) and the fact that hurricanes moving out of the Tropics can still be quite damaging, even though the local potential intensity is small or zero, places limitations on the application of such a method.

Here we elect instead to run a deterministic numerical simulation of hurricane intensity along each synthetic track, using the model developed by Emanuel et al. (2004). This is a simple axisymmetric balance model coupled to an equally simple one-dimensional ocean model. Because the model is phrased in angular momentum coordinates, it yields exceptionally high resolution in the critical eyewall region of the storm. Given a storm track, the model is integrated forward in time to yield a prediction of wind speed. Details of this approach are provided in appendix C.

To generate hurricane wind risk assessments, both track methods are used first to generate large numbers of synthetic tracks. A filter is applied to the track generator to select tracks coming within a specified distance of a point or region of interest (e.g., a city or county). We then run the hurricane intensity model along each

³ In principle, this correction should decrease with the cosine of the latitude, but as storms move to higher latitudes, other steering influences come into play, which introduce errors at least as large as those arising from omitting this effect.

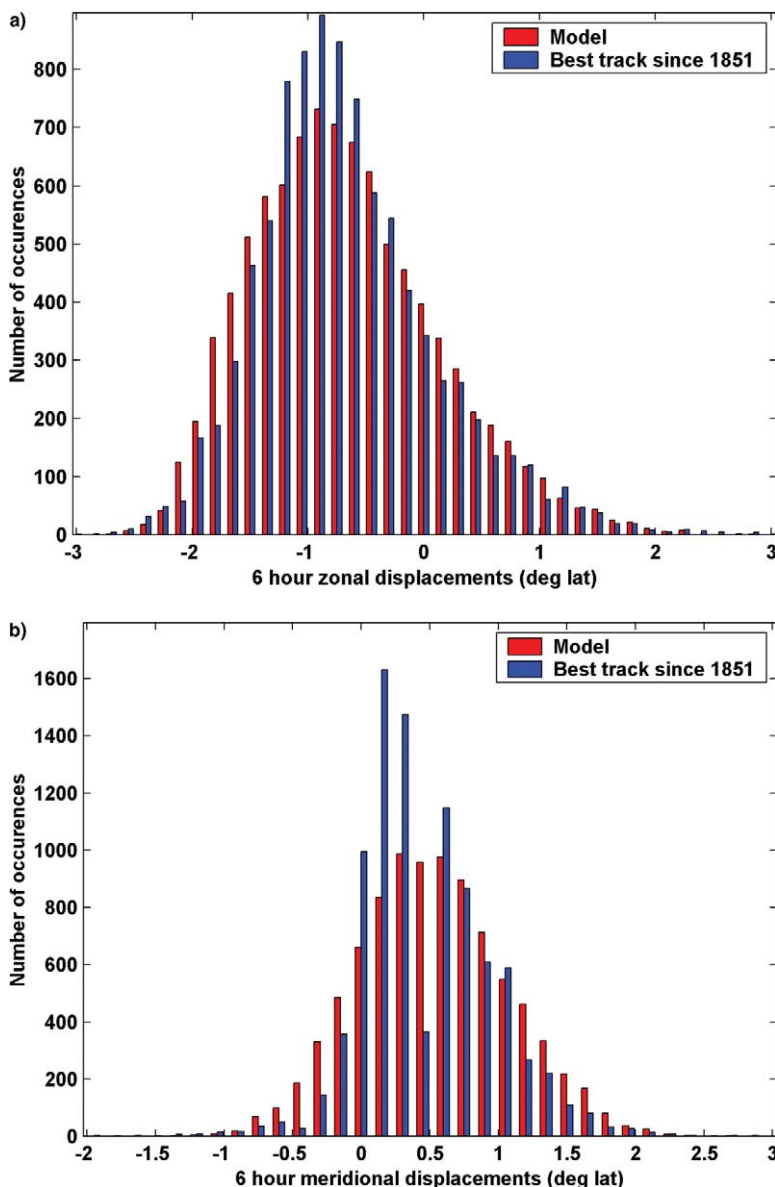


FIG. 2. Same as Fig. 1, but for the second track generation method.

of the selected tracks to produce a history of storm maximum wind speed. The wind shear needed by the intensity model is taken from the same wind fields used to produce the track in the second track method, but separate random wind fields are used in the first. Thus, the storm motion and the vertical wind shear are mutually consistent for tracks generated by the second method, but not for the first.

The coupled deterministic model produces a maximum wind speed and a radius of maximum winds, but the detailed aspects of the radial storm structure are not used, owing to the coarse spatial resolution of the model. Instead, we use an idealized radial wind profile, fitted to the numerical output, to estimate maximum winds at fixed points in space away from the storm center, as described in appendix C. For this purpose, a fraction of the linear translation speed vector is added to the circular vortex wind field to account for some of the observed asymmetry in the overall storm wind pattern.

For each point of interest, the intensity model is run many (an order of 10^4) times to produce exceedence probabilities as a function of wind speed for that point. Both the synthetic track generation methods and the deterministic model are fast enough that it is practical to estimate exceedence probabilities to a comfortable level of statistical significance. We compare such probabilities to those estimated using previously published techniques, and to estimates made directly from historical data as contained in the hurricane database (HURDAT) record (Jarvinen et al. 1984), which is updated through 2002 and revised to include storms from as early as 1851.

RESULTS. To illustrate the capabilities of the present approach, we have created three sets of synthetic hurricanes. The first is random selection of 1000 storms affecting the North Atlantic as a whole. The other two are for cities with very different hurricane climatologies: Miami, Florida, and Boston, Massachusetts. Miami has a relatively rich record of storms, and most of these have not undergone strong interactions with extratropical systems. Boston, at the other extreme, has only had a handful of storms in its history, and many of those can be presumed to have been affected by interactions with extratropical systems.

North Atlantic. Figure 3 compares cumulative frequency distributions of maximum wind speeds achieved in all 1,000 North Atlantic storms created using both of the track generators with all storms in the HURDAT record beginning in 1950, normalized to numbers of events per millennium. The ordinate shows the

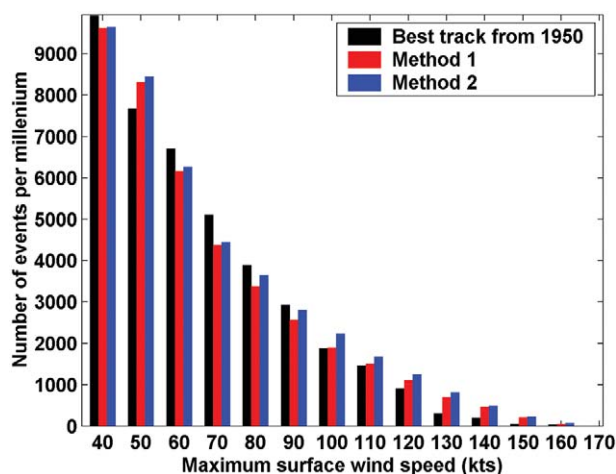


FIG. 3. Cumulative histograms of maximum surface wind speeds achieved along tracks generated by the Markov chain method (red) and the second track generation method (blue), and compared to statistics derived directly from the best-track data (black).

number of events whose wind speeds exceed the value given on the abscissa. The two methods give very similar results, and both slightly overestimate the number of intense storms, but, note that there are few real events to compare to in this latter category.

The cumulative histograms follow the bilinear cumulative frequency distribution of hurricane maximum wind speeds discussed by Emanuel (2000). It is important to note that such distributions are bounded so that there is, in general, a maximum wind speed that can be experienced at any given place. In general, this nearly corresponds to the potential intensity deep in the Tropics, but, especially at higher latitudes, the addition of the storm translation speed allows some maximum wind values to exceed the local potential intensity. As discussed in appendix C, this accounts for part (but not all) of the effect of extratropical transition.

The close correspondence of the intensity statistics shown in Fig. 3, taken together with the good comparison of track displacement statistics shown in Figs. 1 and 2, suggests that this method is a viable approach to assessing hurricane wind risk.

Miami. Miami is an example of a city with a relatively high incidence of hurricanes. To produce annual exceedence probabilities for wind speed, we ran both track models to produce 3,000 tracks each, passing within 100 km of downtown Miami. We then ran the intensity model over each track to accumulate wind statistics for Miami. (Bear in mind that not all storms reach Miami before their wind speeds fall below 13 m s^{-1} and are thus terminated.) To facilitate

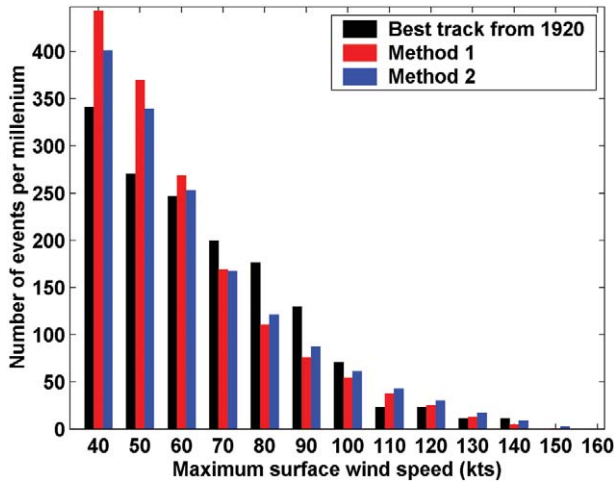


FIG. 4. Cumulative histograms of frequency of exceedence of wind speed within 100 km of downtown Miami. Results from HURDAT data (black) are compared to model data for method 1 (red) and method 2 (blue). There are 29 events in the HURDAT sample versus 3,000 in methods 1 and 2.

comparison with historical hurricane data, we first made histograms of the peak wind speed experienced anywhere within 100 km of downtown Miami in each storm. These are compared to the same statistic derived from HURDAT for both track methods in Fig. 4, expressed as number of events per millennium. In comparing the present results with HURDAT data, bear in mind that there are only 29 HURDAT tracks with maximum winds in excess of 40 kts passing with 100 km of Miami during the period in question, versus the 3,000 tracks used in both methods 1 and 2. We also point out that there are biases in HURDAT arising, for example, from changing conventions in converting between central surface pressure and maximum wind (Landsea 1993). Given these biases and the small absolute sample size, it is likely that the present results are consistent with HURDAT within the statistical significance of the HURDAT-derived histogram. The comparison of the method 1 and method 2 results gives a crude measure of the errors associated with this approach; Fig. 4 shows that they are quite similar in this case.

Figure 5 shows the exceedence probabilities for an area within 100 km of downtown Miami, derived

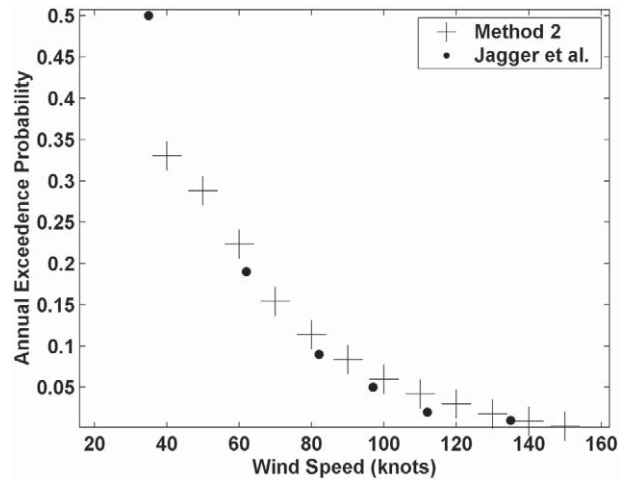
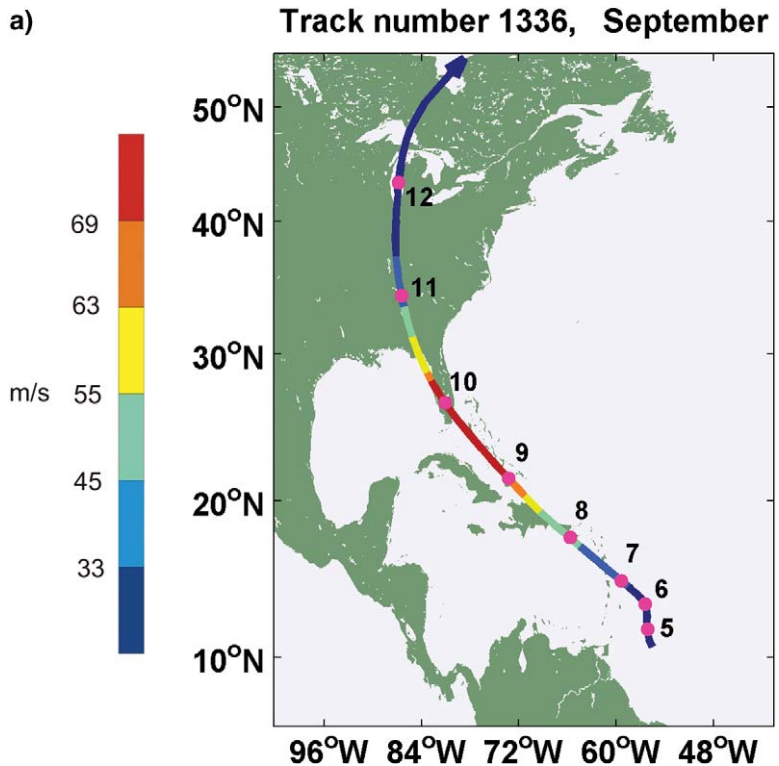


FIG. 5. Annual exceedence probability for downtown Miami from Jagger et al. 2001 (dots) and method 2 (crosses). The former pertains to all Miami-Dade County, while the latter pertains to the maximum wind speed within 100 km of downtown Miami.

using method 2, and compares them to probabilities estimated in the work of Jagger et al. (2001). The latter are for all of Miami-Dade County (which contains the city of Miami), and so should be expected to be a little smaller than the values we estimated using method 2, which covers a somewhat larger area. Jagger et al. (2001) used a maximum likelihood technique based

a)



on a county-level dataset assembled by Jarrell et al. (1992). Our results are remarkably consistent with theirs, considering the large difference between the two techniques and the datasets used.

The track producing the highest wind speed within 100 km of Miami in method 2 is displayed in Fig. 6, together with the evolution of several key quantities along the track. This storm forms on 5 September, and beginning on 7 September accelerates northwestward while intensifying rapidly, achieving a peak wind speed of 169 kts (and minimum central pressure of 892 hPa) just before landfall in south Florida. As shown in Fig. 6b, the peak winds exceed the local potential intensity, owing to the relatively large translation speed of this storm. After crossing southern Florida, this storm weakens to category 3, which it maintains until its second landfall in the Florida Panhandle on 10 September.

Figure 7 shows the tracks of the 30 “worst” events, ranked by the maximum wind speed experienced within 100 km of downtown Miami, for both track methods. Although the statistics of all of the tracks from both methods are similar, there are distinct differences in the tracks of the top 30 events. For example, *none* of the top 30 storms in method 2 approach Miami from west of south, while quite a few method 1 tracks do. This difference is not apparent in a random sample of tracks from both methods. A likely explanation for the differences in the top 30

events is that, in method 2, storms traveling from west of south are likely to be associated with a stronger wind shear and are thus weaker, whereas in method 1 the shear is largely independent of the track direction. This is so even though, in both methods, the shear is climatologically correct.

Boston. Both the power and the limitations of our technique are most evident when applied to places that experience infrequent (but sometimes devastating) storms. In these cases, the historical record may be greatly insufficient to make reasonable risk assessments there from, yet there are still strong incentives to estimate risk. In method 1, the infrequency of storms affects the robustness of the statistics used in the Markov chain track generator, but there are no such limitations to method 2, because the flow variability

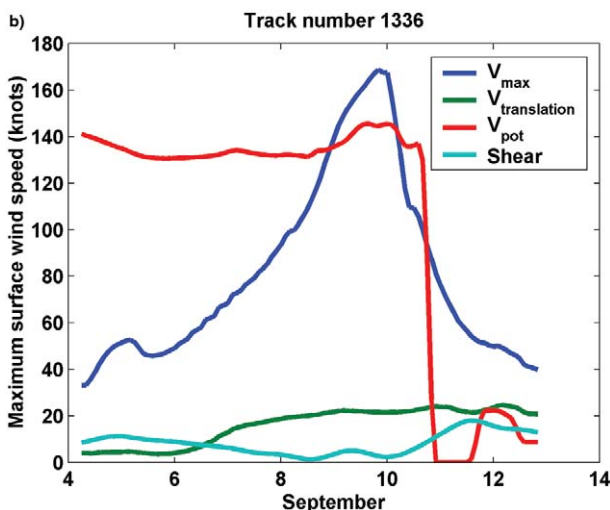


FIG. 6. (a)(FACING PAGE) Track of the most intense of the 3,000 storms passing within 100 km of Miami using method 2, together with (b)(ABOVE) the evolution of maximum wind speed (blue), potential intensity (red), translation speed (green), and 250–850-hPa wind shear magnitude (light blue). The colors in (a) correspond to maximum wind speeds given by scale at left, and the numbers are dates in September.

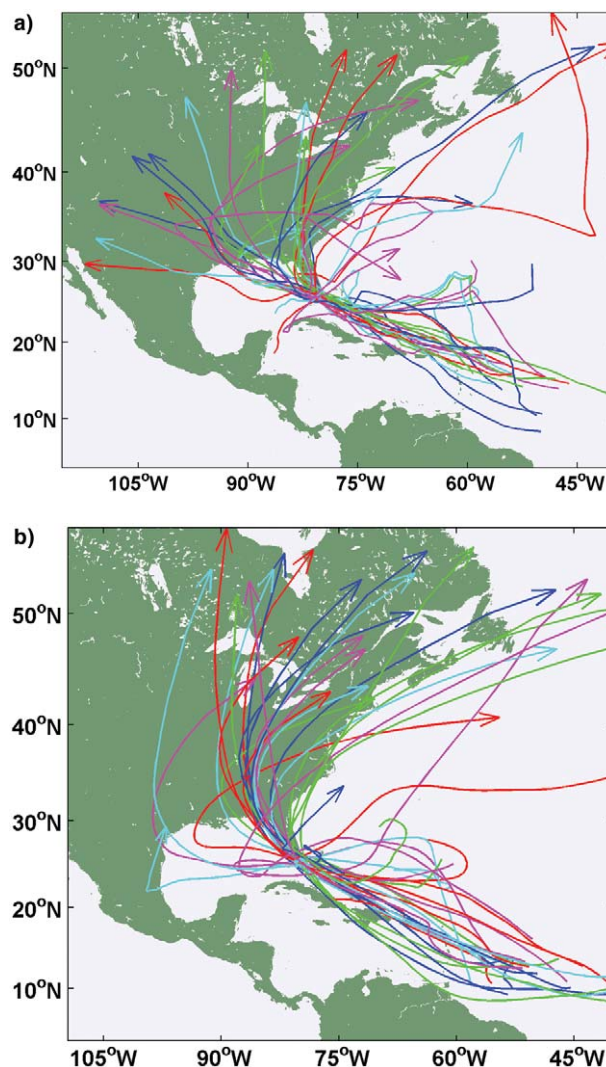


FIG. 7. Thirty tracks yielding the highest peak winds within 100 km of Miami from (a) method 1 and (b) method 2.

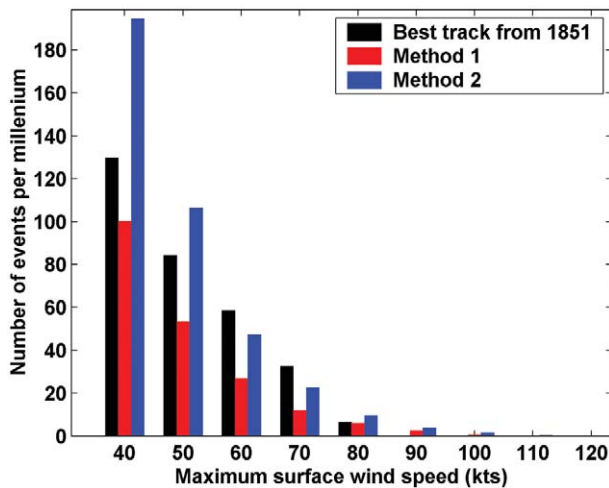


FIG. 8. Cumulative histograms of frequency of exceedence of wind speed within 100 km of downtown Boston. Results from HURDAT data (black) are compared to model data for method 1 (red) and method 2 (blue). There are 27 events in the HURDAT sample versus 3,000 in methods 1 and 2.

is no less realistically represented by reanalysis data in high latitudes than in low latitudes; indeed, the flow at high latitudes may be more robust. On the other hand, the proposition that tropical cyclones move with some weighted vertical mean flow plus a correction becomes more dubious as extratropical transition occurs.

The model used to predict intensity evolution has no explicit treatment of extratropical interactions, though some of this effect in surface winds may be captured, as discussed in appendix C, by adding the translation speed to the azimuthal winds.

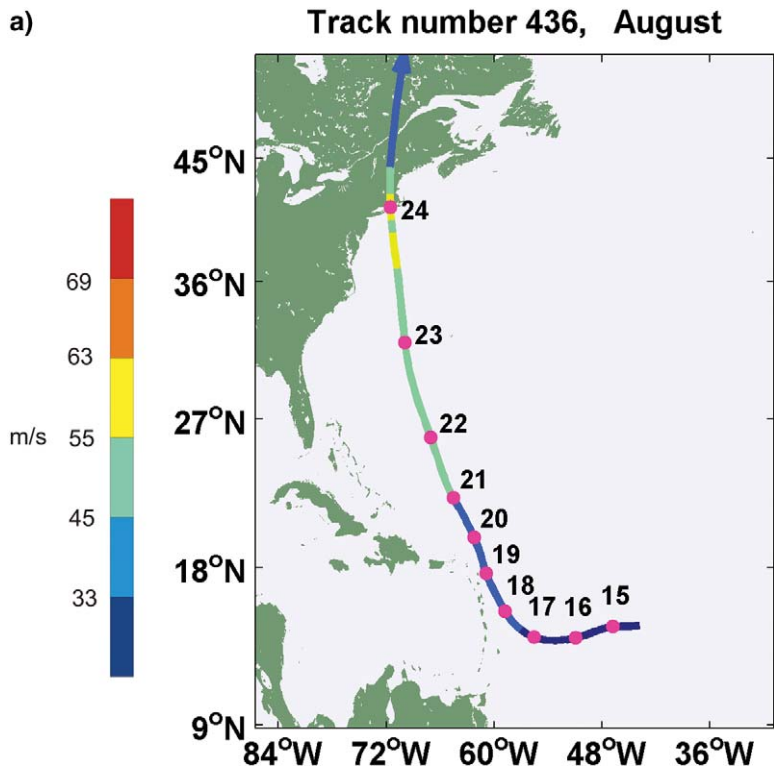
Cumulative frequency distributions of the maximum wind speed within 100 km of downtown Boston from both methods are compared to HURDAT and to each other in Fig. 8. The HURDAT distributions are based on only 27 events, so caution should be used in interpreting the results. There are large differences in low-intensity events between the two methods, with a substantially larger number of weak events when using method 2. This may be owing to artificially large survival rates of weak storms in method 2, in which there are more slow-moving storms that affect Boston. The two

methods are somewhat more consistent in frequencies of high-intensity events, though there are still generally more in method 2.

The track of the most intense storm affecting downtown Boston in method 2, with peak winds of 84 kts, is shown in Fig. 9, together with the evolution of key quantities along the track. Much of the high wind speed in the Northeast is attributable to the rapid forward movement of the storm. As shown in Fig. 10, 93 of the 100 most intense storms affecting Boston in method 2 originate in the tropical Atlantic—6 form in the Caribbean, and 1 originates in the Gulf of Mexico and travels across peninsular Florida. Also shown in Fig. 10 is the track of Hurricane Bob of 1991, the most recent storm to produce hurricane-force winds within 100 km of Boston. Its track falls well within the envelope of the 100 most intense storms of method 2.

SUMMARY. Dealing with natural hazards, from creating building codes to setting insurance premiums and planning for evacuations and relief efforts, depends on an accurate assessment of risk. Estimates of hurricane wind risk based directly on the historical record suffer from the overall scarcity of events, particularly in regions that experience infrequent but sometimes devastating storms. Even in regions suffering a high frequency of events, fitting standard

a)



probability distribution functions to observations may be inaccurate at the high-intensity end of the distribution, which is based on sparse data but accounts for a disproportionate amount of injury, loss of life, and destruction. Here we have attempted to circumvent some of these limitations by synthesizing large numbers of storm tracks and then running a deterministic hurricane intensity model along each track. This has the advantage of ensuring that the intensity of storms conforms broadly to the underlying physics, including the natural limitations imposed by potential intensity, ocean coupling, vertical wind shear, and landfall.

To synthesize hurricane tracks, we developed and tested two quite independent methods. The first constructs each track as a Markov chain whose probability of vector displacement change depends on position, season, and the previous 6-h vector displacement, with the statistics determined by standard distribution functions fitted to observed track data. The second postulates that hurricanes move with a weighted average of upper- and lower-tropospheric flow plus a “beta drift” correction. The flow is generated using synthetic time series of wind whose monthly mean, variance, and covariance conform to statistics derived from reanalysis data and whose kinetic energy obeys the observed ω^{-3} frequency distribution characteristic of geostrophic turbulence. Shear derived from these synthetic flows is used as input to the intensity model in both track methods. The statistics of storm motion produced by both methods conform well to observed displacement statistics and to each other.

Wind exceedence probabilities for Miami, Florida, generated using both track methods agree well

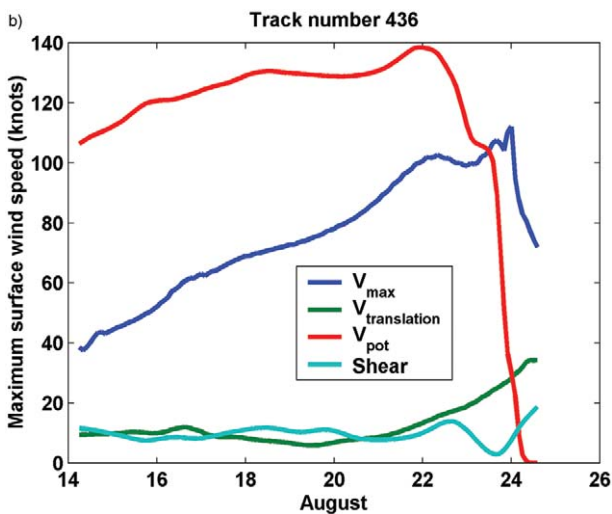


FIG. 9. As in Fig. 6, but for the most intense of the 3,000 storms in the sample of storms affecting downtown Boston, using method 2. Dates are in August.

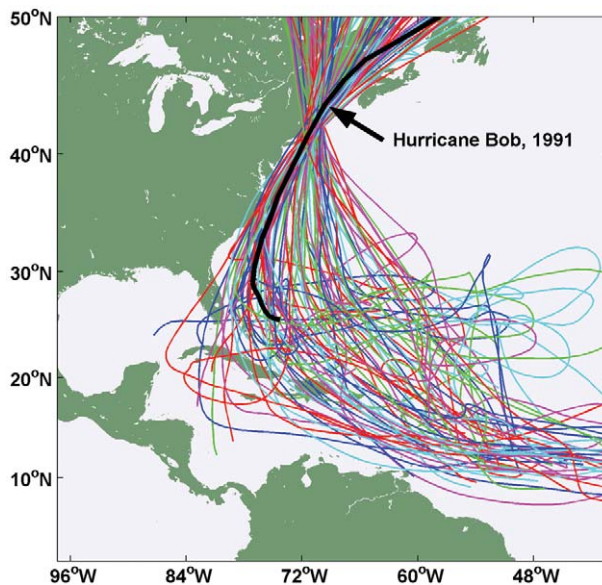


FIG. 10. Tracks of the 100 most intense of the 3,000 storms in the sample of storms affecting downtown Boston, using method 2. Shown for comparison (in black) is the observed track of Hurricane Bob of 1991.

with each other, with histograms based directly on HURDAT, and with estimates stemming from previously published research. Wind probabilities at Boston, Massachusetts, however, reveal the comparative strengths and weaknesses of the two methods. Storms affecting high-latitude locations are almost always influenced by the interaction of tropical and extratropical systems; such an interaction is represented in the present work only by adding the storm’s translation speed to its tangential wind. Our second track method therefore cannot capture the effects of nonlinear interactions between tropical and extratropical systems, whereby either or both system may be intensified, giving a translation speed in excess of that which would have been produced by a strictly linear superposition of the preexisting systems. This effect is, however, represented in our first track method, because it is reflected in the displacement statistics used in the Markov chain. On the other hand, the wind shear affecting storms generated by the first track method is independent of the storm motion. This may yield possibly large biases in tracks taken by the most severe events, as illustrated by Fig. 7. In addition, the second method may be used to generate tracks wherever the climatological reanalysis winds are deemed reliable, whereas the quality of tracks generated using the first method may be compromised in regions with little historical data. Both methods rely on an accurate estimate of the space–time distribution of storm generation.

To the extent that one has reliable characterizations of the interannual to interdecadal variation of atmospheric winds, for example, owing to El Niño (Gray 1984), the Atlantic Multidecadal Oscillation (Goldenberg et al. 2001), or the North Atlantic Oscillation (Elsner et al. 2000), and tropical cyclogenesis distributions, or a prediction of how they might change in a future climate, the second track method (and, to a lesser extent the first) can be used to estimate corresponding changes in hurricane wind risk. This is a subject of ongoing research by our group. One factor that is known to influence hurricane intensity is upper-ocean thermal variability. We are working to characterize the statistics of such variability and to incorporate this in our wind risk models.

ACKNOWLEDGMENTS. The authors are grateful for very helpful reviews by Chris Landsea and two anonymous reviewers.

APPENDIX A: SYNTHETIC TRACK GENERATION USING MARKOV CHAINS.

Our statistical approach to constructing synthetic tracks can be divided into three phases. First, a smooth, discrete space–time genesis probability distribution is constructed from the HURDAT (Jarvinen et al. 1984) track database and genesis events are sampled from this distribution. (For this purpose, we use data only from 1970 and later, when global storm detection by satellite is regarded as being complete.) Second, each sample is integrated forward in 6-h steps as a *Markov chain* (Lange 2003), using translation speed and direction and their rates of change as state variables. Transition probabilities for the Markov chain are constructed using variable-resolution, kernel-smoothed nonparametric densities conditioned on a prior state, time, and position.

The Markov chain model is motivated by the fact that the temporal autocorrelation spectra of speed and angles suggest meaningful correlation length scales of no longer than three (6 h) time units, indicating a colored process that is well modeled as a Markov process (Lange 2003). We chose these state variables because we found that they can better represent track continuity than a latitude–longitude–time parameterization. We use kernel-smoothed, variable-resolution representations (Wand and Jones 1994), motivated by the necessity to produce distributions that are not prone to sampling failures.

Tracks are terminated using two criteria: the first is a termination probability density function (PDF) constructed in a similar manner to the genesis PDF from HURDAT and, the second is when searches at multiple space–time resolutions fail to provide evidence for a transition. We continue tracks over land and cold water, because our intensity estimator will naturally allow storms to decay under such circumstances. All of the Atlantic track data were derived from the HURDAT track database maintained by the NOAA Tropical Prediction Center, covering the period of 1851–2002. For the purpose of deriving track-displacement statistics, we used data from this entire period, though comparison with calculations using only post-1970 data show some differences (see appendix B). We have also used TPC and JTWC track data to generate tracks in other ocean basins, but do not report on those results here.

Details of this track synthesizer are presented in the online supplement (DOI:10.1175/BAMS-87-3-Emanuel) to this paper. Here we present some statistical analyses of tracks generated using this method.

Figure A1 compares a sample of 60 tracks generated by this technique to a random sample of HURDAT tracks. In general, the shape of the tracks is similar, though the synthetic tracks are a bit smoother. Figure 1

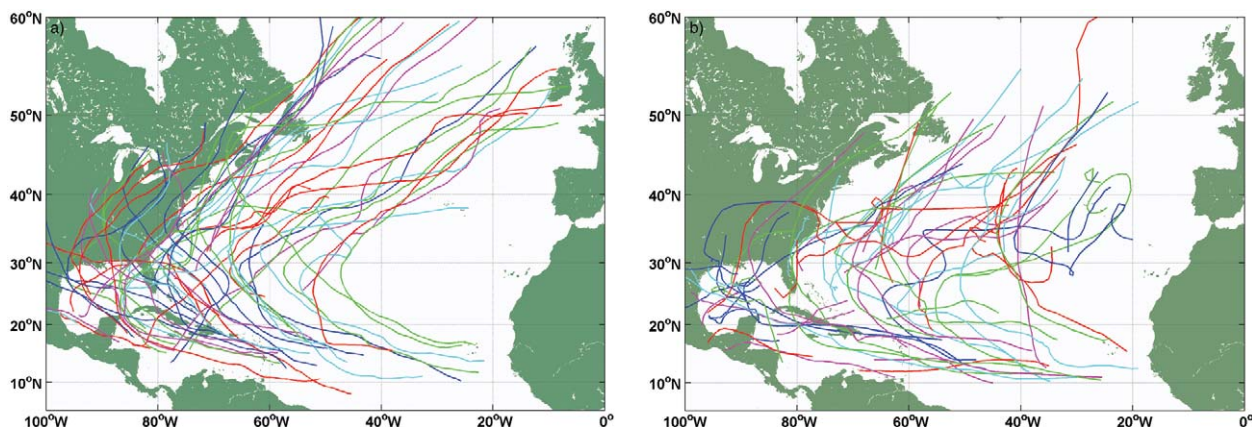


FIG. A1. Sixty random tracks from (a) the Markov chain method, and (b) HURDAT data.

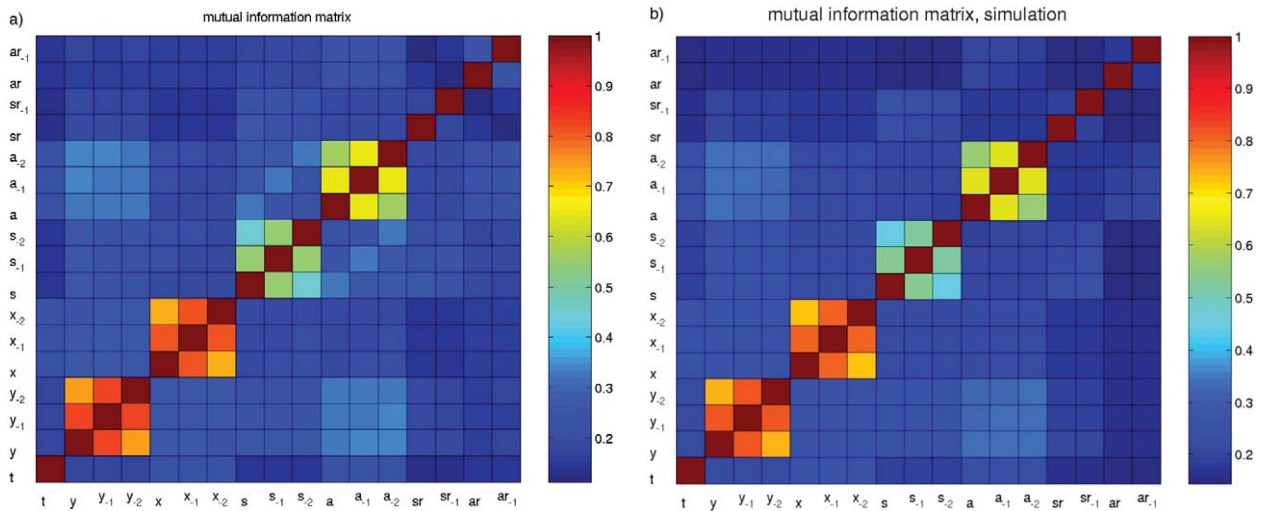


FIG. A2. The normalized mutual information between variables used to represent (a) a hurricane from HURDAT and (b) from tracks synthesized using Markov chains. The mutual information is a measure of statistical similarity; here it is color coded according to the colorbar at right. The variables are time t , x , y , track direction a , translation speed s , time rate of change of angle, ar , and rate of change of translation speed sr . The subscripts denote time lags; thus, s_{-6} represents translation speed 6 h earlier.

compares the statistics of 6-h zonal and meridional displacements of 1000 synthetic tracks to all 1289 tracks in the HURDAT data for a region of the North Atlantic bounded by 10° and 30° N latitude and 80° and 30° W longitude. We choose this region as one in which the synthetic tracks are likely to be maintained in an intensity model, as opposed to regions like that just east of eastern North America, where many synthetic tracks have had large trajectories over land and are therefore unlikely to be maintained by an intensity model. The comparison is excellent, as one might expect, given that the statistics of the HURDAT data have been used to construct the synthetic tracks.

Another source of comparison was obtained from an experiment for quantifying the statistical dependence between the variables involved in the statistical model. The panel on the left of Fig. A2 is a matrix consisting of rates of change of direction and speed, and direction, speed, position, and time, with subscripts indicating lag (read from top to bottom or from right to left). This matrix is symmetric and the color reflects the normalized mutual information (Li et al. 2003) given by

$$N(X_i, X_j) = \sqrt{\frac{I(X_i, X_j)}{\text{MIN}[H(X_i), H(X_j)]}}$$

Here, I is the mutual information (Shannon 1948), and H is the entropy (Cover and Thomas 1991), defined as

$$H(X) = -\sum_i P(X = x_i) \ln[P(X = x_i)]$$

$$H(X|Y) = \sum_i P(Y = y_i) H(X|y_i)$$

$$I(X, Y) = H(X) - H(X|Y) = H(Y) - H(Y|X).$$

The matrix for HURDAT shows a pattern of dependency that is replicated with good fidelity by our simulation.

APPENDIX B: TRACK GENERATION FROM SYNTHETIC WIND TIME SERIES.

The object here is to produce synthetic time series of wind used both to generate hurricane tracks, under the assumption that storms move with some vertical mean wind plus a drift term, and to generate realistically varying environmental wind shear along the track of each storm to use in the storm intensity model. So to keep matters simple, we choose to use winds only at the 850- and 250-hPa levels. This choice is motivated by the finding of DeMaria and Kaplan (1994) that the wind shear between these two levels is well correlated with hurricane intensity change, and the shear between these levels is also used in the operational application of the coupled hurricane intensity prediction model described in appendix C. The motion of each storm is modeled as a weighted average of flow at these two levels, plus a beta-drift correction. This is similar to the “deep” version of the beta and advection model (Marks 1992), which uses a weighted average flow between 850 and 200 hPa. It should be noted that inclusion of levels other than at 850 and 200 hPa may slightly improve

the results, based on experience with the beta and advection model.

We begin by generating a synthetic time series of the zonal wind component at 250 hPa, modeled as a Fourier series in time with a random phase and designed to have the observed monthly mean and variance from the mean. Using the same technique, we then generate a synthetic time series of the meridional wind component at 250 hPa, but, in addition to the constraints placed on the zonal wind, we constrain this time series to have the observed covariance with the 250-hPa zonal wind. Finally, synthetic time series of both of the 850-hPa wind components are generated and constrained to have the observed means, variances, and covariances with their respective components at 250 hPa and with each other. (We do not constrain the 850-hPa wind components to have the observed covariance with the opposite components at 250 hPa.) Note that we do not explicitly model spatial correlations of the mean flow. In effect, we assume that the time scale over which a hurricane traverses typical length scales associated with time-varying synoptic-scale systems is large compared to the time scale of fluctuations at a fixed point in space. Notwithstanding this, each storm will, of course, feel the effects of spatial variability of the monthly mean flow and its variance. Details of this method are presented in the “Generation of synthetic time series of 250- and 850-hPa flow” section of the online supplement to this paper (DOI:10.1175/BAMS-87-3-Emanuel).

Monthly means, variances, and covariances were calculated using 40 yr of data from the NCEP–NCAR reanalysis dataset (Kalnay et al. 1996). Given time series of the flow at 250 and 850 hPa, it is straightforward to calculate the magnitude of the 850–250-hPa shear used by the hurricane intensity model described in appendix C. Hurricane tracks were synthesized from a weighted mean of the 250- and 850-hPa flow plus a correction for beta drift:

$$\mathbf{V}_{\text{track}} = \alpha \mathbf{V}_{850} + (1 - \alpha) \mathbf{V}_{250} + \mathbf{V}_{\beta}, \quad (\text{B1})$$

where \mathbf{V}_{850} and \mathbf{V}_{250} are the vector flows at the two pressure levels, synthesized using the technique described in the online supplement to this paper (DOI:10.1175/BAMS-87-3-Emanuel), α is a constant weight, and \mathbf{V}_{β} is a constant-vector beta-drift term. The weight α and the vector beta drift \mathbf{V}_{β} are chosen somewhat subjectively to optimize comparisons of the synthesized and observed displacement statistics. In the present work, we take $\alpha = 0.8$, $\mu_{\beta} = 0 \text{ m s}^{-1}$, and $v_{\beta} = 2.5 \text{ m s}^{-1}$.

Given $\mathbf{V}_{\text{track}}$ from (1), we integrate

$$\frac{d\mathbf{x}}{dt} = \mathbf{V}_{\text{track}}$$

forward in time (using a 30-min forward time step) to find the position vector \mathbf{x} along each track. The reanalysis mean fields, variances, and covariances are then linearly interpolated in space and time to the new position (and new date), assigning the monthly mean to the 15th day of each month, and the position equation is stepped forward again. Unlike the previous track generation method, we do not have the problem of running into regions where the generating statistics become poor, so instead we terminate the track if its maximum (storm relative) winds fall below 13 m s^{-1} , if it travels outside a predefined latitude–longitude box, or after 30 days, whichever happens first. For Atlantic storms, the bounding box is defined by 4° and 50°N , 5° and 110°W .

Figure B1 shows an example of 60 randomly selected tracks produced by this method; these may be compared to 60 tracks generated by the first method (Fig. A1a) and to 60 randomly selected historical tracks (Fig. A1b). In general, this track generation method produces somewhat more variable tracks than those produced with the Markov chain, with more tracks executing loops, etc. The zonal and meridional 6-h displacement statistics for 1000 tracks in a region of the North Atlantic bounded by 10° and 30°N latitude and 80° and 30°W longitude are shown in Fig. 2 and compared to the statistics of all 1289 historical tracks. Figure 2 should also be compared to Fig. 1, showing the same statistics for the first track method. The second track method produces 6-h displacement distributions that are slightly too broad when compared to either the historical tracks or the tracks produced by the first method.

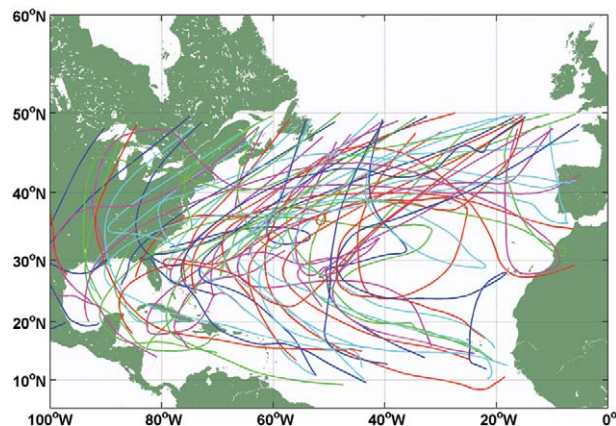


FIG. B1. Sixty randomly selected tracks using the second track generation method.

Several factors may explain the inferior statistics of the second track method. First, the synthetic time series of winds used to generate the tracks are only approximations of real wind fields. Second, the notion that hurricanes move with some weighted mean of the 250- and 850-hPa wind plus a beta-drift correction is itself a rather crude approximation, especially considering that the beta drift is variable and that other factors, such as vertical shear, contribute to the storm's alteration of the background potential vorticity distribution. Not all flows are conducive to tropical cyclone maintenance, and while the statistics that underlie the first track generation method no doubt reflect this, the second method has no way of accounting for this. But when we run our intensity model along each track, those going through flows unfavorable to hurricane maintenance will naturally terminate, and this may be expected to affect the track statistics. We have recalculated the displacement statistics after running the intensity model, and in the latitude–longitude box described in the preceding paragraph, the statistics are not appreciably different. Finally, it may be that the HURDAT displacement statistics are themselves biased, especially before the satellite era, when large segments of the open-ocean tracks had to be inferred from sparse observations. To assess this effect, we recalculated the displacement statistics using HURDAT data only after 1970 (and renormalizing the count of the synthesized tracks). The result for the zonal displacements, shown in Fig. B2, shows a better match, suggesting that the earlier HURDAT data are indeed biased. (The results for the meridional displacements also show improvement.)

APPENDIX C: DETERMINISTIC MODELING OF HURRICANE INTENSITY. To estimate the intensity of hurricanes following the synthetic tracks, we run a deterministic numerical simulation of hurricane intensity along each track, using the model developed by Emanuel et al. (2004). This is a simple axisymmetric balance model coupled to an equally simple one-dimensional ocean model. The model is phrased in angular momentum coordinates, yielding exceptionally high resolution (as high as 1 km) in the critical eyewall region of the storm. Given a storm track, the model is integrated forward in time to yield a prediction of wind speed. Because the atmospheric

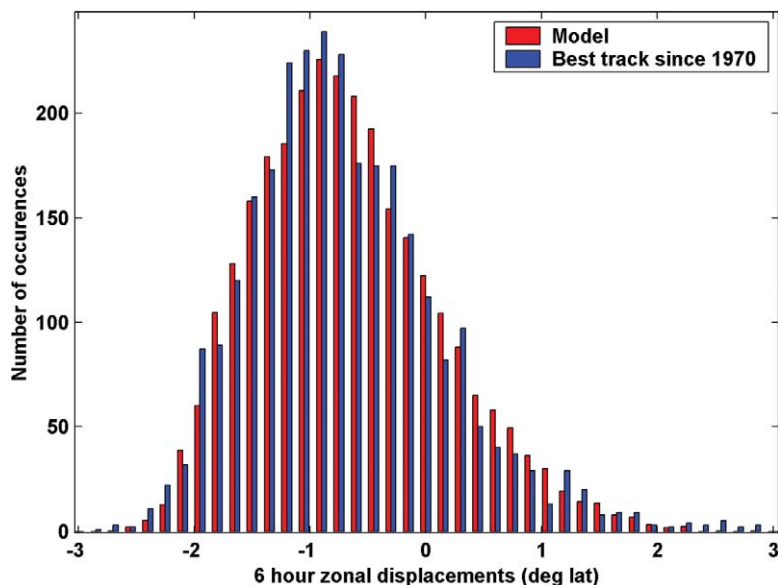


FIG. B2. Same as Fig. 2a, but using only post-1970 HURDAT tracks.

model is axisymmetric, it cannot explicitly account for the important influence of environmental wind shear, and this must therefore be represented parametrically; the procedure for doing this is described in detail in Emanuel et al. (2004). Bathymetry and topography are included, and landfall is represented by reducing the surface enthalpy exchange coefficient, depending on the elevation of the land. The model is run quasi-operationally at NHC and JTWC and gives forecasts that are comparable in skill to other forecast methods (Emanuel and Rappaport 2000).

In addition to the storm track, the model requires estimates of potential intensity, upper-ocean thermal structure, and environmental wind shear along the track. In this application, we use monthly mean climatological potential intensity calculated from NCEP–NCAR reanalysis data, linearly interpolated to the storm position and in time to the date in question. As shown by Emanuel et al. (2004), use of real-time potential intensity offers only a marginal improvement over the climatological means. As in the quasi-operational model, we use monthly mean climatological upper-ocean thermal structure obtained from Levitus (1982). On the other hand, Emanuel et al. (2004) showed that upper-ocean thermal variability can have a significant influence on hurricane intensity in this model. Although we do not account for such variability here, we intend to include this in future work, using sea surface altimetry data to help quantify the climatological variability of the upper ocean.

Vertical wind shear is an important influence on hurricane intensity, in this model as in nature. Here

we apply the wind shear calculated from synthetic time series of winds at 850 and 250 hPa, as described in appendix B. In the case of the first track method, using Markov chains to generate tracks, this wind shear will be independent of the track displacements (though, of course, it will vary with position along the track and with season), but, in the second method, the same wind fields are used to generate tracks and shear, so the two will be mutually consistent.

In the quasi-operational application of the intensity model, the integration is initialized by matching the time evolution of the intensity to that of the observed storm prior to the initialization time. Here we simply prescribe an initial intensity of 15 m s^{-1} and an initial intensification rate of about $6 \text{ m s}^{-1} \text{ day}^{-1}$. If and when the predicted (storm relative) maximum drops below 13 m s^{-1} , the storm is assumed to have dissipated and the integration is discontinued. In rare cases, the storm may reach the end of a track before this happens.

The rate of genesis of tropical cyclones is taken from climatology, as previously described, and is independent of the wind field taken at the beginning of the synthetic time series whose generation is described in detail in the “Generation of synthetic time series of 250- and 850-hPa flow” section of the online supplement to this paper (DOI:10.1175/BAMS-

87-3-Emanuel). While it is unrealistic to assume that storms will be generated under conditions of large shear, the intensity model will quickly kill storms under these conditions. To save integration time, we regenerate the random wind series whenever the vertical shear at the genesis point exceeds 12 m s^{-1} .

The intensity model takes, on the average, about 15 s of wall-clock time to run a single track on a typical workstation computer. Thus, it is feasible to run a large number of tracks. For the purposes of this paper, we chose a limited number of sites of interest and then created a large number (on the order of 10^4) of synthetic tracks passing within a specified radius of the site in question, running the intensity model along each track. (For high-latitude sites, such as Boston, only a small fraction of storms survive to influence the site, and this is accounted for in accumulating wind statistics for the site.)

To estimate wind speeds at fixed points in space, it is necessary to estimate the radial structure of the storm’s wind field. While the intensity model does predict such structure, it is not particularly realistic, owing to the coarse radial resolution outside the eye-wall, and we elect instead to use a parametric radial wind profile fitted to the model-predicted maximum wind speed and radius of maximum winds. We use the parametric form developed by Emanuel (2004):

$$V^2 = V_m^2 \left(\frac{r_0 - r}{r_0 - r_m} \right)^2 \left(\frac{r}{r_m} \right)^{2m} \left[\frac{(1-b)(n+m)}{n+m \left(\frac{r}{r_m} \right)^{2(n+m)}} + \frac{b(1+2m)}{1+2m \left(\frac{r}{r_m} \right)^{2m+1}} \right],$$

where V_m is the maximum wind speed, r is radius, r_m is the radius of maximum winds, r_0 is an outer radius at which the winds vanish, and b , m , and n are parameters governing the shape of the wind profile. Here we take $r_0 = 1200 \text{ km}$, $b = 1/4$, $m = 1.6$, and $n = 0.9$. (Here, V_m and r_m are supplied by the intensity model.) The liberal estimate of r_0 only affects the outer structure of the vortex and thus should only affect probability assessments at low wind speeds. The structure given by (C1) is similar to that of the parametric vortex developed by Holland (1980).

To this axisymmetric wind field we add a fraction of the storm’s translation velocity in the direction of the storm’s motion. We find, empirically, that relatively good agreement with historical data is obtained using 60% of the translation speed.

A weakness of the present approach is that dynamical interactions with extratropical systems are specifically excluded. Were such interactions linear, and were both the tropical cyclone and the extratropical systems with which it interacts quasigeostrophic, then the wind fields of all of the systems could be linearly superposed and the extratropical interaction would be accounted for by having added the translation speed to the wind speed. But extratropical transition is no doubt strongly nonlinear, and the circulation around the tropical cyclone may be expected, under some circumstances, to enhance the amplitude of extratropical potential vorticity anomalies, so one might expect that the present method would not deal adequately with extreme cases of extratropi-

cal transition. A case in point is the New England Hurricane of 1938, whose translation velocity at landfall is estimated to have been around 30 m s^{-1} (Minsinger 1988). It is hardly credible that such a velocity would result from the weighted mean of the 850- and 250-hPa flow that is used to calculate translation velocities by the second track method presented in this study, though it would presumably be represented in the track statistics used in the Markov chain approach.

For each storm, we calculated the maximum wind speed experienced at the site of interest as well as the maximum wind speed experienced within a fixed distance from that site. Because the model was tuned for maximum winds reported by NHC, we take these winds to represent 1-min averages at an altitude of 10 m. By summing over the total number of events, annual wind exceedance probabilities and return periods can be estimated and these can be compared to estimates based directly on historical data such as HURDAT.

REFERENCES

- Casson, E., and S. Coles, 2000: Simulation and extremal analysis of hurricane events. *Appl. Stat.*, **49**, 227–245.
- Chu, P.-S., and J. Wang, 1998: Modeling return periods of tropical cyclone intensities in the vicinity of Hawaii. *J. Appl. Meteor.*, **37**, 951–960.
- Cover, T. M., and J. A. Thomas, 1991: *Elements of Information Theory*. Wiley-Interscience, 542 pp.
- Darling, R. W. R., 1991: Estimating probabilities of hurricane wind speeds using a large-scale empirical model. *J. Climate*, **4**, 1035–1046.
- Davies, T. V., 1948: Rotatory flow on the surface of the earth. Part I. Cyclostrophic motion. *Philos. Mag.*, **39**, 482–491.
- DeMaria, M., and J. Kaplan, 1994: A statistical hurricane intensity prediction scheme (SHIPS) for the Atlantic basin. *Wea. Forecasting*, **9**, 209–220.
- Elsner, J. B., K.-B. Liu, and B. Kocher, 2000: Spatial variations in major U.S. hurricane activity: Statistics and a physical mechanism. *J. Climate*, **13**, 2293–2305.
- Emanuel, K. A., 2000: A statistical analysis of tropical cyclone intensity. *Mon. Wea. Rev.*, **128**, 1139–1152.
- , 2004: Tropical cyclone energetics and structure. *Atmospheric Turbulence and Mesoscale Meteorology*, E. Federovich, R. Rotunno, and B. Stevens, Eds., Cambridge University Press, 165–192.
- , and E. Rappaport, 2000: Forecast skill of a simplified hurricane intensity prediction model. Preprints, *24th Conf. on Hurricanes and Tropical Meteorology*, Ft. Lauderdale, FL, Amer. Meteor. Soc., CD-ROM, 6A.5.
- , C. DesAutels, C. Holloway, and R. Korty, 2004: Environmental control of tropical cyclone intensity. *J. Atmos. Sci.*, **61**, 843–858.
- Georgiou, P. N., A. G. Davenport, and P. J. Vickery, 1983: Design wind speeds in regions dominated by tropical cyclones. *J. Wind Eng. Ind. Aerodyn.*, **13**, 139–152.
- Goldenberg, S. B., C. W. Landsea, A. M. Mestas-Nuñez, and W. M. Gray, 2001: The recent increase in Atlantic hurricane activity: Causes and implications. *Science*, **293**, 474–479.
- Gray, W. M., 1984: Atlantic seasonal hurricane frequency. Part I: El Niño and 30 mb quasi-biennial oscillation influences. *Mon. Wea. Rev.*, **112**, 1649–1668.
- Holland, G., 1980: Analytic model of the wind and pressure profiles in hurricanes. *Mon. Wea. Rev.*, **108**, 1212–1218.
- , 1983: Tropical cyclone motion: Environmental interaction plus a beta effect. *J. Atmos. Sci.*, **40**, 328–342.
- Jagger, T., J. B. Elsner, and X. Niu, 2001: A dynamic probability model of hurricane winds in coastal counties of the United States. *J. Appl. Meteor.*, **40**, 853–863.
- Jarrell, J. D., P. J. Hebert, and B. M. Mayfield, 1992: Hurricane experience levels of coastal county populations—Texas to Maine. NOAA Tech. Memo. NWS NHC 31, 152 pp.
- Jarvinen, B. R., C. J. Neumann, and M. A. S. Davis, 1984: A tropical cyclone data tape for the North Atlantic Basin, 1886–1983: Contents, limitations, and uses. NOAA Tech. Memo. NWS/NHC 22, 21 pp.
- Kalnay, E., and Coauthors, 1996: The NCEP/NCAR 40-Year Reanalysis Project. *Bull. Amer. Meteor. Soc.*, **77**, 437–471.
- Landsea, C., 1993: A climatology of intense (or major) Atlantic hurricanes. *Mon. Wea. Rev.*, **121**, 1703–1714.
- Lange, K., 2003: *Applied Probability*. Springer, 320 pp.
- Levitus, S., 1982: *Climatological Atlas of the World Ocean*. National Oceanic and Atmospheric Administration Prof. Paper 13, 173 pp. and 17 microfiche.
- Li, M., Chen, X. Li, B. Ma, and P. Vitanyi, 2004: The similarity metric. *Inf. Theory*, **50**, 3250–3264.
- Marks, D. G., 1992: The beta and advection model for hurricane track forecasting. NOAA Tech. Memo. NWS NMC 70, 89 pp.
- Minsinger, W. E., 1988: *The 1938 Hurricane: An Historical and Pictorial Summary*. Greenhill Books, 128 pp.
- Murnane, R. J., and Coauthors, 2000: Model estimates of hurricane wind speed probabilities. *Eos, Trans. Amer. Geophys. Union*, **81**, 433–438.

- Neumann, C. J., 1987: The national hurricane center risk analysis program (HURISK). NOAA Tech. Memo. NWS NHC 39, 56 pp.
- Pielke, R. A. J., and C. W. Landsea, 1998: Normalized U.S. hurricane damage, 1925–1995. *Wea. Forecasting*, **13**, 621–631.
- Rossby, C.-G., 1949: On a mechanism for the release of potential energy in the atmosphere. *J. Meteor.*, **6**, 164–180.
- Shannon, C. E., 1948: A mathematical theory of communication. *Bell Syst. Technol. J.*, **27**, 379–423; 623–656.
- Vickery, P. J., P. F. Skerjil, and L. A. Twisdale, 2000: Simulation of hurricane risk in the U.S. using empirical track model. *J. Struct. Eng.*, **126**, 1222–1237.
- Wand, M. P., and M. C. Jones, 1994: *Kernal Smoothing*. Chapman and Hall, 224 pp.
- Watson, C. C., and M. E. Johnson, 2004: Hurricane loss estimation models: Opportunities for improving the state of the art. *Bull. Amer. Meteor. Soc.*, **85**, 1713–1726.